Sign-reversal of the in-plane resistivity anisotropy in hole-doped iron pnictides

E. C. Blomberg,[1,2] M. A. Tanatar,[1] R. M. Fernandes,[3,4] Bing Shen,[5] Hai-Hu Wen,[5,6] J. Schmalian,[7] and R. Prozorov[1,2,*]

[1] *The Ames Laboratory, Ames, IA 50011, USA*
[2] *Department of Physics and Astronomy, Iowa State University, Ames, IA 50011, USA*
[3] *Department of Physics, Columbia University, New York, New York 10027, USA*
[4] *Theoretical Division, Los Alamos National Laboratory, Los Alamos, NM, 87545, USA*
[5] *Institute of Physics, Chinese Academy of Sciences, Beijing 100190, P. R. China*
[6] *National Laboratory of Solid State Microstructures and Department of Physics, Nanjing University, Nanjing 210093, P. R. China*
[7] *Institut fr Theorie der Kondensierten Materie, Karlsruher Institut fr Technologie, D-76131 Karlsruhe, Germany*

(Dated: February 21, 2012)

The in-plane anisotropy of the electrical resistivity across the coupled orthorhombic and magnetic transitions of the iron pnictides has been extensively studied in the parent and electron-doped compounds. All these studies universally show that the resistivity ρ_a across the long orthorhombic axis a_O - along which the spins couple antiferromagnetically below the magnetic transition temperature - is smaller than the resistivity ρ_b of the short orthorhombic axis b_O, i. e. $\rho_a < \rho_b$. Here we report that in the hole-doped compounds $Ba_{1-x}K_xFe_2As_2$, as the doping level increases, the resistivity anisotropy initially becomes vanishingly small, and eventually changes sign for sufficiently large doping, i. e. $\rho_b < \rho_a$. This observation is in agreement with a recent theoretical prediction that considers the anisotropic scattering of electrons by spin-fluctuations in the orthorhombic/nematic state.

INTRODUCTION

The undoped and moderately-doped AFe$_2$As$_2$ (A=Ca, Sr, Ba, Eu) compounds undergo a tetragonal-to-orthorhombic transition at a temperature T_s, which is either accompanied or followed by stripe-type magnetic order below $T_N \leq T_s$ [1], with in-plane ordering vector $(\pi, 0)$ or $(0, \pi)$. Since superconductivity in these compounds is induced upon suppression of the structural and magnetic orders by doping or pressure, it is natural to assume that magnetic fluctuations play an important role in the pairing interaction. Therefore, it is of great importance to understand not only the origin of the magnetism of these materials, but also how it affects the normal state properties. Interestingly, experiments in different types of materials suggest a close relationship between unconventional superconductivity and spin-fluctuation scattering [2].

In the phase diagram of the iron pnictides, the magnetic and structural transition lines always follow each other [3, 4]. To describe the close relationship between these two orders, two alternative scenarios have been proposed. One scenario considers that the structural transition is a secondary consequence of an emergent Ising-nematic phase, which appears in the paramagnetic state due to the interplay between magnetic fluctuations and the doubly-degenerate character of the striped magnetic phase [5–8]. Another scenario considers that spontaneous orbital ordering triggers the structural transition and removes the intrinsic frustration of the striped magnetic state, which then appears at lower temperatures [9–12].

Since the nematic, orbital, and orthorhombic orders all break the tetragonal symmetry of the system, it is difficult to decide between the different scenarios only in the qualitative level. Thus, it is fundamental to experimentally investigate the macroscopic properties of this anisotropic state thoroughly. In this context, the resistivity anisotropy is an important benchmark, since several concurring mechanisms for anisotropic transport are present, such as Fermi surface reconstruction in the magnetically ordered state [13–15], electronic reconstruction due to orbital order [11, 12, 16–18], and anisotropic scattering by spin fluctuations [19].

Experimentally, the resistivity anisotropy can be studied in crystals which have been detwinned by the application of an uniaxial stress or strain [15, 20], see Ref.[21] for review. A very unique picture was observed in the parent and electron-doped materials [15, 20] $A(Fe_{1-x}TM_x)_2As_2$ (TM=Co, Ni, Cu): counter-intuitively, the resistivity in the antiferromagnetic state is larger along the direction of ferromagnetic chains (short orthorhombic b_O direction) than along the direction of antiferremagnetic spin chains (long orthorhombic a_O direction). The anisotropy remains finite well above the orthorhombic transition temperature of the unstressed sample, suggesting the presence of a large nematic susceptibility in the tetragonal phase, in agreement with elastic modulus measurements [22].

In our initial study [15], we concluded that the anisotropy in the magnetically ordered state can be well understood using band structure calculations. Despite the good agreement of this conclusion with recent Shubnikov-de Haas oscillations measurements [23] and detailed transport analysis [24] in detwinned crystals of undoped $BaFe_2As_2$, the authors of Ref.[23] argued that with this mechanism it would be very difficult to explain

the large in-plane anisotropy $\rho_b/\rho_a \sim 2$ observed in Co-doped samples. Alternative explanations focused on the unequal occupation of d_{xz} and d_{yz} orbitals in the antiferromagnetic phase as the origin of the anisotropic transport [13, 24].

While these discussions focused on the effects of the reconstructed band structure on the resistivity anisotropy, the temperature dependence of $\Delta\rho \equiv \rho_b - \rho_a$, and also optical conductivity data [25], reveal the importance of anisotropic scattering as well. The resistivity anisotropy in all parent compounds [26] is maximum at T_s, where both the orthorhombic lattice distortion and the magnitude of the magnetic moment are minimum. This motivated a model where scattering by spin fluctuations, which are anisotropic in the nematic/orthorhombic state, plays a fundamental role in determining the properties of the resistivity anisotropy [19]. An interesting prediction of this model is that the resistivity anisotropy in hole-doped materials should change sign for sufficiently high doping.

Indeed, $\Delta\rho$ was reported to be very different in electron-doped and hole-doped $BaFe_2As_2$ [27], where it becomes vanishingly small for moderate hole-doping levels. Motivated by the prediction of Ref. [19], in this paper we report a systematic study of the in-plane resistivity anisotropy for a broader doping range of underdoped $Ba_{1-x}K_xFe_2As_2$ (BaK122), from $x = 0$ (the parent compound) to compositions close to optimal doping, $x = 0.34$ and $T_c = 38$ K. We find a change in the sign of the resistivity anisotropy for $x > 0.235$, confirming the fundamental role of anisotropic spin-fluctuation scattering in the description of the resistivity anisotropy. Furthermore, we also find that the temperature dependence of the anisotropy below T_N (i.e. in the magnetically ordered state) qualitatively changes for similar doping levels, with $|\Delta\rho|$ monotonically increasing with cooling. This feature suggests that the magnetically reconstructed Fermi surface may undergo profound changes as positive charge carriers are introduced in the parent compound.

EXPERIMENTAL

Single crystals of BaK122 with sizes up to 7x7x1 mm^3 were grown from FeAs flux as described in Ref.[28]. Potassium content in the samples was determined using electron probe microanalysis with wavelength dispersive spectroscopy (WDS), see [29] for details. Samples had typical dimensions of 0.5 mm wide, 2 to 3 mm long, and 0.05 mm thick, and were cut from cleaved slabs along the tetragonal [110] direction (which becomes either the orthorhombic a_O or b_O axis below T_s). Optical imaging was performed on the samples while mounted on a cold finger in a continuous flow liquid helium cryostat (allowing precise temperature control in the 5K to 300K range) using a *Leica DMLM* microscope.

Sample images in polarized light were used for visualization of the structural domains [30] and initial sample selection was based on the clarity of domains in the image. Selected samples were mounted for four-probe electrical resistivity measurements, with contacts made by soldering 50 μm Ag wires using low-resistance Sn soldered contacts [31]. The first resistivity measurement on each sample was carried out using a flexible wire arrangement with no strain applied to the sample (free standing state). Samples were then mounted on a brass horseshoe straining device, and strain was applied through the voltage contact wires by deformation of the horseshoe, see Ref.[15, 26] for the details of measurements. Strain in this configuration is applied along the tetragonal [110] axis, which then becomes the long orthorhombic a_O axis upon cooling below T_s. The current leads are arranged such that they do not apply additional strain. The strain was incrementally increased and, for each increment, temperature-dependent resistivity measurements were made and the domain structure imaged to determine the completeness of detwinning. When no structural domains were visible the sample was considered detwinned. The strain needed to completely detwin the samples is estimated to be in the 10 to 20 MPa range based on our previous work [32]. Because of the small magnitude of the resistivity changes, detailed attention was given to optical imagaing to determine when the samples were detwinned.

RESULTS

Polarized Microscopy

In Fig. 1. we show polarized light images of the area between the potential contacts in BaK122 crystals used in this study, with $x = 0.108$ (non-superconducting), $x = 0.202$ ($T_c = 10$K), $x = 0.235$ ($T_c = 26$K), and $x = 0.259$ ($T_c = 28$K). Images were taken on cooling at a temperature slightly above T_s and at base temperature. The highest contrast is observed when the sample is aligned with the [110] tetragonal direction at 45° to the polarization direction of incident light (parallel and perpendicular to the orthorhombic a_O in different domains). The contrast of domain images depends on the quality of the surface and the homogeneity of the samples. Domains are observed for samples with $x \approx 0.26$, but are not observed for samples with higher doping level, $x = 0.34$, which do not show any features in $\rho(T)$ associated with the structural transition, see Fig. 2.

Resistivity

Temperature-dependent resistivity, see Fig. 2, was first measured in the samples without strain. In the twinned

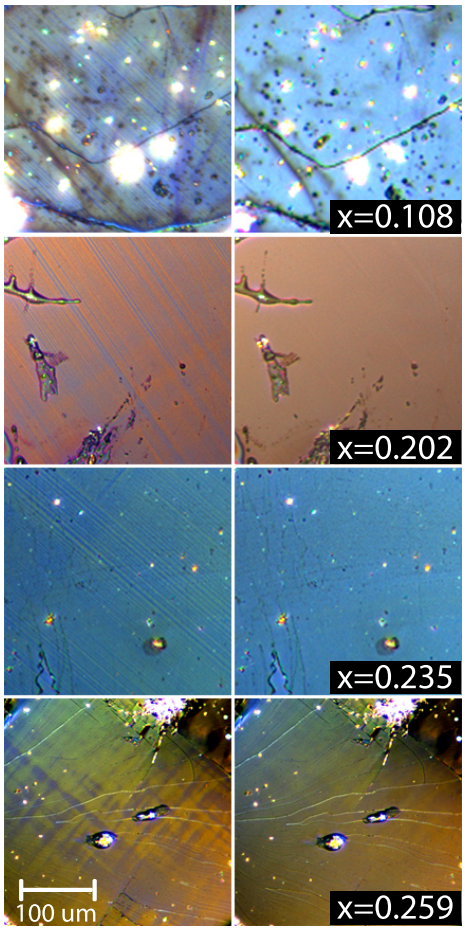

FIG. 1. (Color Online) Polarized light microscopy of BaK122 samples with doping levels as shown in the panels. Images were taken at temperatures just above the tetragonal-to-orthorhombic structural transition ($T > T_s$, right) and 5K ($T < T_s$, left), the latter showing formation of structural domains due to four different orientations of the a_O and b_O axes. The difference in color of the domains is due to spectral dependence of bireflectance, depending on the angle between the a_O direction and the polarization plane of incident white light. Since bireflectance is proportional to the orthorhombic distortion, the contrast naturally vanishes in the tetragonal phase (right panels).

crystal we may assume a roughly equal population of domains with the a_O axis parallel to the current direction and domains with the b_O axis parallel to it. Therefore, the resistivity in the free-standing crystals is close to the average value of the resistivities of the two orthorhombic axes, $\rho_t(T) = [\rho_a(T) + \rho_b(T)]/2$.

Our previous studies showed that when crystals are strained until no domains are visible in polarized microscopy, about 90% of the bulk of the sample displays the domain whose orthorhombic a_O axis is oriented along the direction of the strain and, consequently, parallel to the current. Therefore, in the detwinned state, we are predominantly measuring the a_O axis resistivity,

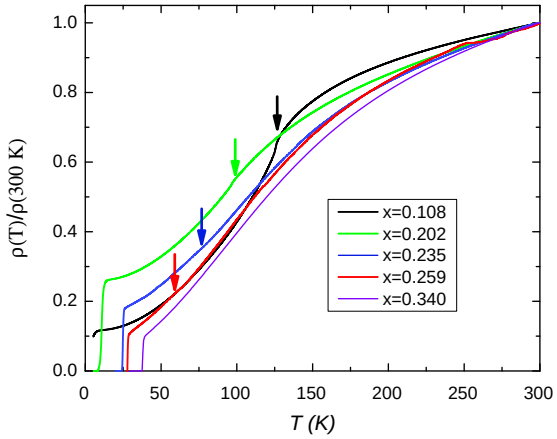

FIG. 2. (Color Online) Temperature-dependent resistivity along the orthorhombic a_O-axis, ρ_a, for samples of BaK122 with five different potassium doping levels in the strain-free, twinned, state. The curves are shown using normalized plots, $\rho_a(T)/\rho_a(300K)$. Arrows indicate the transition temperatures and were determined by the maximum in the derivative of the resistivity and from polarized optical microscopy.

ρ_a. Using this, we calculate the b axis resistivity from $\rho_b(T) = 2\rho_t(T) - \rho_a(T)$. The measured ρ_a and calculated ρ_b are shown for samples with $x = 0.202$ and $x = 0.235$ in Fig. 3. Note that the application of strain has the opposite effect on the resistivity of the two samples, with $\rho_a < \rho_b$ for $x = 0.202$ (and all samples with smaller x), but $\rho_a > \rho_b$ for samples with $x = 0.235$ and $x = 0.259$. In the bottom panel of Fig. 3, we plot the temperature-dependent anisotropy ratio ρ_b/ρ_a for all the samples studied, including those with $x = 0$.

We summarize our results in Fig. 4. In the top panel, we combine the phase diagram determined from magnetization and neutron scattering measurements on polycrystals of BaK122 [33] and single crystals of BaCo122, with our measurements for the structural transition temperature T_s and the superconducting transition temperature T_c. The former was determined from the maximum of the resistivity derivative $d\rho/dT$ and from polarized microscopy, while the latter was determined from the transition mid-point. In the middle panel, we summarize the measurements of the in-plane resistivity anisotropy in electron- and hole-doped materials, using our current results as well as previously published data. Specifically, we plot the maximum value of the temperature-dependent anisotropy for each case. It is clear that the data from different groups are in good semi-quantitative agreement, with minor differences coming most likely from poor control of residual strain in the different experimental setups used for sample detwinning. The bottom panel displays the theoretical result of the model of Ref. [19], and will be explained in the discussion section.

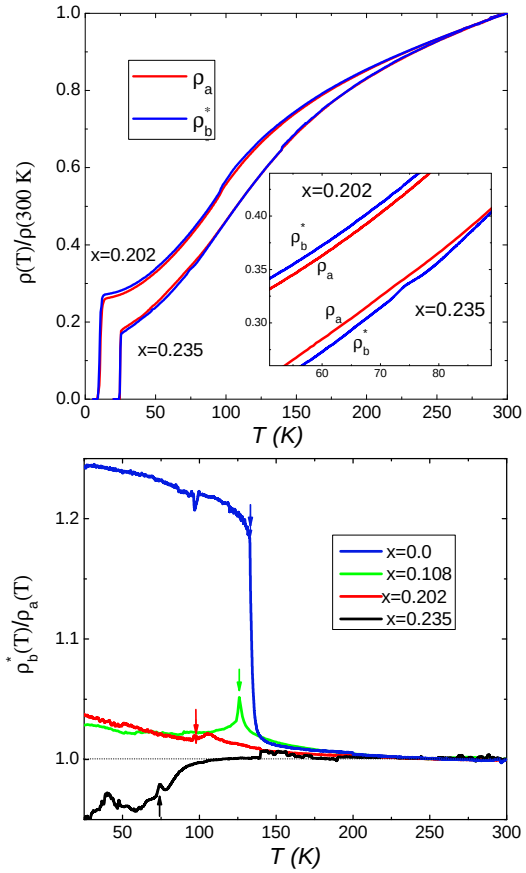

FIG. 3. (Color Online) Top panel. Normalized temperature-dependent resistivity, $\rho(T)/\rho(300K)$, for BaK122 samples $x = 0.202$ and $x = 0.235$. The red lines show the resistivity along the a_O-axis (ρ_a), the blue lines show ρ_b. The inset shows a zoom of the structural transition, with clear reversal of anisotropy from $\rho_b > \rho_a$ for $x = 0.202$ to $\rho_b < \rho_a$ for $x = 0.235$. Bottom panel shows the temperature-dependent anisotropy, $\rho_b/\rho_a(T)$, for samples with different K-doping levels. .

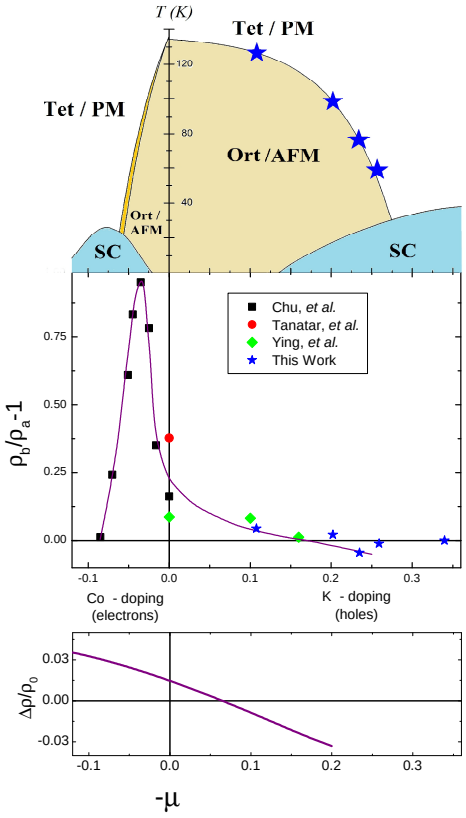

FIG. 4. (Color Online) **Top panel**. Unified phase diagram of $BaFe_2As_2$ for the cases of electron (Co-substitution of Fe) and hole (K-substitution of Ba) dopings, showing the structural, magnetic, and superconducting transition lines (after Refs.[33, 36]). Data points (blue stars) are the measurements extracted in this study. **Middle panel**. Maximum in-plane anisotropy, $\rho_b/\rho_a(T)$, as function of electron- and hole-doping. For both types of doping the anisotropy vanishes with suppression of the orthorhombic distortion close to optimal doping, however, it reveals a steep maximum in electron-doped compounds (x=0.035 Co doping) versus a sign change in hole-doped materials with zero-crossing around x=0.17. Data points for the middle panel were taken from the following references: J. H. Chu *et al.* (black squares) Ref. [20], M. A. Tanatar *et al.* (red circle) Ref. [15], and J. J. Ying *et al.* (green diamonds) Ref. [27]. **Bottom panel**. Theoretical calculation of the maximum resistivity anisotropy $\Delta\rho$ (in units of the residual resistivity due to impurity-scattering ρ_0) in the *paramagnetic-nematic phase*, as described in Ref. [19], as function of the chemical potential μ (in units of the Fermi energy). Here, $\mu > 0$ corresponds to electron-doping whereas $\mu < 0$ corresponds to hole-doping.

Discussion

The measured resistivity anisotropy of all electron-doped and parent compounds is such that $\rho_b/\rho_a > 1$ for all temperatures. In $Ba_{1-x}K_xFe_2As_2$, this property persists for slight to moderate potassium hole-doping, ranging from $\rho_b/\rho_a \approx 1.2$ to 1.5, down to 1.02 for samples with $x = 0.202$. For samples with $x = 0.235$, this decreasing trend of ρ_b/ρ_a culminates in a sign-change of the resistivity anisotropy $\Delta\rho = \rho_b - \rho_a$, with $\rho_b/\rho_a \approx 0.956$. Upon increasing doping even further, the anisotropy eventually vanishes due to the crossing into tetragonal phase.

Since the sign-change happens above the magnetic transition temperature, as evidenced in Fig. 3, we first analyze our results without invoking the reconstruction of the Fermi surface due to long-range magnetic order. There are two main mechanisms that render the resistivity anisotropic in the paramagnetic/orthorhombic phase: orbital order [11, 12] and anisotropic scattering by spin-fluctuations [19, 34]. As pointed out by both Refs. [18] and [12], orbital order alone, as observed experimentally[16], gives the wrong sign of the resistivity anisotropy in the parent and electron-doped samples, indicating that the main contribution is coming from spin-fluctuation scattering.

In the model discussed in Ref. [19], the scattering by spin fluctuations becomes anisotropic below the orthorhombic/nematic transition temperature T_s because the fluctuations around one of the two possible stripe ordering vectors, $(\pi, 0)$ and $(0, \pi)$, become stronger than the fluctuations around the other ordering vector. In this case, and when impurity scattering is also present, only electrons near the hot spots associated with the selected ordering vector are strongly scattered by spin fluctuations. Then, the sign of the resistivity anisotropy is determined by the projections along a_O and b_O of the Fermi velocity at the these hot spots. Roughly, if the hot-spot Fermi velocity has a larger component along the b_O direction, electrons will be more strongly scattered by spin fluctuations when they travel along this direction, and $\rho_b > \rho_a$. We can then understand the sign-change in $\Delta\rho \equiv \rho_b - \rho_a$ as function of doping in a qualitative way: since doping changes the relative sizes of the hole and electron pockets of the Fermi surface, it also changes the position (and therefore the Fermi velocity) of the hot spots. In particular, electron-doping brings the hot spots closer to the b_O axis, implying $\rho_b > \rho_a$, while hole-doping brings the hot spots closer to the a_O axis, yielding $\rho_b < \rho_a$. To illustrate this general feature of the model, in the bottom panel of Fig. 4 we plot the calculated maximum anisotropy $\Delta\rho$ as function of doping in the nematic-paramagnetic phase, considering the particular case explored in Ref. [19] of critical magnetic fluctuations and large impurity scattering.

A qualitative comparison with the experimental data in the middle panel of Fig. 4 shows that this model indeed captures not only the sign-change of the resistivity anisotropy, but also the asymmetry between electron-doping and hole-doping. However, the model does not seem to capture the peak of the maximum $\Delta\rho$ at an intermediate electron-doping level. Since the theory is valid only in the paramagnetic state, for $T > T_N$, it suggests that this observed peak is related to the anisotropic Fermi-surface reconstruction in the magnetically-ordered state. Indeed, as pointed out in [14], the doping level corresponding to this peak in the maximum anisotropy coincides with a Lifshitz transition that was found in comparative ARPES/thermopower measurements [35]. In particular, in this Lifshitz transition, a small hole-like reconstructed pocket disappears from the Fermi surface.

This point sheds light on another interesting feature of our resistivity anisotropy measurements. As shown in the bottom panel of Fig. 3, the temperature-dependent anisotropy ratio ρ_b/ρ_a is maximum at T_s for both the parent compound and the slightly hole-doped composition $x = 0.108$. However, for the two other samples with higher doping levels, $|\rho_b - \rho_a|$ increases monotonically as the temperature is decreased. One possibility, in view of the behavior observed in the electron-doped compounds, is that this change in the temperature-dependence of the resistivity anisotropy reflects a change in the topology of the reconstructed Fermi surface as function of hole-doping. Such a change should also impact other macroscopic properties, and therefore could be verified by other experimental probes. On the theoretical side, it is interesting to note that Ref. [18], investigating the Drude weights along a_O and b_O in the magnetically ordered phase, found different signs of the resistivity anisotropy depending on the properties of the reconstructed Fermi surface.

Summarizing, we observe a change in the sign of the in-plane resistivity anisotropy when going from electron-doped to hole-doped $BaFe_2As_2$ compounds, in agreement with the general theoretical predictions of the anisotropic spin-fluctuation scattering model of Ref. [19]. The temperature dependence of the anisotropy below T_N also changes and becomes monotonically increasing with cooling, suggesting that changes in the reconstructed Fermi surface may also take place with hole doping.

ACKNOWLEDGEMENTS

We thank E. Abrahams for fruitiful discussions. Work at the Ames Laboratory was supported by the Department of Energy-Basic Energy Sciences under Contract No. DE-AC02-07CH11358. Work in China was supported by the Ministry of Science and Technology of China, project 2011CBA00102. R.M.F. thanks the valuable support from the NSF Partnerships for International Research and Education (PIRE) program.

* Corresponding author: prozorov@ameslab.gov

[1] C. de la Cruz, Q. Huang, J. W. Lynn, J. Y. Li, W. Ratcliff, J. L. Zarestky, H. A. Mook, G. F. Chen, J. L. Lou, N. L. Wang, and P. C. Dai, Nature **453**, 899 (2008).
[2] L. Taillefer, Ann. Rev. Condens. Matter Phys. **1**, 51 (2010).
[3] R. M. Fernandes, D. K. Pratt, W. Tian, J. Zarestky, A. Kreyssig, S. Nandi, M. G. Kim, A. Thaler, N. Ni, P. C. Canfield, R. J. McQueeney, J. Schmalian, and A. I. Goldman, Phys. Rev. B **81**, 140501(R) (2010).
[4] S. Nandi, M. G. Kim, A. Kreyssig, R. M. Fernandes, D. K. Pratt, A. Thaler, N. Ni, S. L. Bud'ko, P. C. Canfield, J. Schmalian, R. J. McQueeney, and A. I. Goldman, Phys. Rev. Lett. **104**, 057006 (2010).
[5] Q. Si and E. Abrahams, Phys. Rev. Lett. **101**, 076401 (2008); E. Abrahams and Q. Si, J. Phys.: Condens. Matter **23**, 223201 (2011).
[6] C. Fang, H. Yao, W.-F. Tsai, J. Hu, and S. A. Kivelson, Phys. Rev. B **77**, 224509 (2008).
[7] C. Xu, M. Muller, and S. Sachdev, Phys. Rev. B **78**, 020501(R) (2008).
[8] R. M. Fernandes, A. V. Chubukov, J. Knolle, I. Eremin, and J. Schmalian, Phys. Rev. B **85**, 024534 (2012).
[9] F. Kruger, S. Kumar, J. Zaanen, J. van den Brink, Phys. Rev. B **79**, 054504 (2009).

[10] W. G. Yin, C. C. Lee, and W. Ku, Phys. Rev. Lett. **105**, 107004 (2010).

[11] C.-C. Chen, J. Maciejko, A. P. Sorini, B. Moritz, R. R. P. Singh, and T. P. Devereaux, Phys. Rev. B **82**, 100504 (2010).

[12] W. Lv and P. Phillips, Phys. Rev. B **84**, 174512 (2011).

[13] Z. P. Yin, K. Haule and G. Kotliar, Nature Physics **7**, 294 (2011)

[14] Hsueh-Hui Kuo, Jiun-Haw Chu, Scott C. Riggs, Leo Yu, Peter L. McMahon, Kristiaan De Greve, Yoshihisa Yamamoto, James G. Analytis, and Ian R. Fisher, Phys. Rev. B **84**, 054540 (2011).

[15] M. A. Tanatar, E. C. Blomberg, A. Kreyssig, M. G. Kim, N. Ni, A. Thaler, S. L. Bud'ko, P. C. Canfield, A. I. Goldman, I. I. Mazin, and R. Prozorov, Phys. Rev. B **81**, 184508 (2010).

[16] M. Yi, D. Lu, J.-H. Chu, J. G. Analytis, A. P. Sorini, A. F. Kemper, B. Moritz, S.-K. Mo, R. G. Moore, M. Hashimoto Proceedings of the National Academy of Sciences 108, 6878 (2011)

[17] T. Shimojima et al., Phys. Rev. Lett. 104, 057002 (2010); Yeongkwan Kim, Hyungju Oh, Chul Kim, Dongjoon Song, Wonsig Jung, Beomyoung Kim, Hyoung Joon Choi, Changyoung Kim, Bumsung Lee, Seunghyun Khim, Hyungjoon Kim, Keehoon Kim, Jongbeom Hong, and Yongseung Kwon Phys. Rev. B 83, 064509 (2011)

[18] E. Bascones, M. J. Calderon, and B. Valenzuela, Phys. Rev. Lett. **104**, 227201 (2010)

[19] R. M. Fernandes, E. Abrahams, and J. Schmalian, Phys. Rev. Lett. **107**, 217002 (2011)

[20] Jiun-Haw Chu, J. G. Analytis, K. De Greve, P. L. McMahon, Z. Islam, Y. Yamamoto, and I. R. Fisher, Science **329**, 824 (2010).

[21] I. R. Fisher, L. Degiorgi, and Z. X. Shen, Rep. Prog. Phys. **74**, 124506 (2011).

[22] R. M. Fernandes, L. H. VanBebber, S. Bhattacharya, P. Chandra, V. Keppens, D. Mandrus, M. A. McGuire, B. C. Sales, A. S. Sefat, and J. Schmalian, Phys. Rev. Lett. 105, 157003 (2010).

[23] Taichi Terashima, Nobuyuki Kurita, Megumi Tomita, Kunihiro Kihou, Chul-Ho Lee, Yasuhide Tomioka, Toshimitsu Ito, Akira Iyo, Hiroshi Eisaki, Tian Liang, Masamichi Nakajima, Shigeyuki Ishida, Shin-ichi Uchida, Hisatomo Harima, and Shinya Uji, Phys. Rev. Lett. **107**, 176402 (2011).

[24] S. Ishida, T. Liang, M. Nakajima, K. Kihou, C. H. Lee, A. Iyo, H. Eisaki, T. Kakeshita, T. Kida, M. Hagiwara, Y. Tomioka, T. Ito, and S. Uchida Phys. Rev. B 84, 184514 (2011)

[25] A. Lucarelli, A. Dusza, A. Sanna, S. Massidda, J.-H. Chu, I.R. Fisher, L. Degiorgi, New J. Phys. **14**, 023020 (2012).

[26] E. C. Blomberg, M. A. Tanatar, A. Kreyssig, N. Ni, A. Thaler, Rongwei Hu, S. L. Bud'ko, P. C. Canfield, A. I. Goldman, and R. Prozorov Phys. Rev. B **83**, 134505 (2011)

[27] J.J. Ying, X.F. Wang, T. Wu, Z.J. Xiang, R.H. Liu, Y.J. Yah, A.F. Wang, M. Zhang, G.J. Ye, P. Cheng, J.P. Hu, X.H. Chen, Phys. Rev. Lett. 107, 067001 (2011).

[28] H. Q. Luo, Z. S. Wang, H. Yang, P. Cheng, X. Zhu, and H.-H. Wen, Supercond. Sci. Technol. **21**, 125014 (2008).

[29] M. A. Tanatar, E. C. Blomberg, Hyunsoo Kim, Kyuil Cho, W. E. Straszheim, Bing Shen, Hai-Hu Wen, R. Prozorov, arXiv:1106.0533

[30] M. A. Tanatar, A. Kreyssig, S. Nandi, N. Ni, S. L. Bud'ko, P. C. Canfield, A. I. Goldman, and R. Prozorov Phys. Rev. B **79**, 180508 (2009)

[31] M. A. Tanatar, N. Ni, S. L. Bud'ko, P. C. Canfield, and R. Prozorov, Supercond. Sci. Technol. **23**, 054002 (2010).

[32] E. C. Blomberg, A. Kreyssig, M. A. Tanatar, R. Fernandes, M. G. Kim, A. Thaler, J. Schmalian, S. L. Bud'ko, P. C. Canfield, A. I. Goldman, and R. Prozorov, arXiv:1111.0997

[33] S. Avci, Omar Chmaissem, Eugene A. Goremychkin, Stephan Rosenkranz, John-Paul Castellan, Duck-Young Chung, Ilya S. Todorov, John A. Schlueter, Helmut Claus, Mercouri G. Kanatzidis, Aziz Daoud-Aladine, Dmitry Khalyavin, Raymond Osborn, Phys. Rev. B **83**, 172503 (2011).

[34] S. Liang, G. Alvarez, C. Sen, A. Moreo, and E. Dagotto, arXiv:1111.6994.

[35] C. Liu, T. Kondo, R. M. Fernandes, A. D. Palczewski, E. D. Mun, N. Ni, A. N. Thaler, A. Bostwick, E. Rotenberg, J. Schmalian, S. L. Bud'ko, P. C. Canfield, and A. Kaminski, Nature Phys. **6**, 419 (2010).

[36] D. K. Pratt, M. G. Kim, A. Kreyssig, Y. B. Lee, G. S. Tucker, A. Thaler, W. Tian, J. L. Zarestky, S. L. Bud'ko, P. C. Canfield, B. N. Harmon, A. I. Goldman, and R. J. McQueeney Phys. Rev. Lett. **106**, 257001 (2011)

[37] M. A. Tanatar, N. Ni, G. D. Samolyuk, S. L. Bud'ko, P. C. Canfield, and R. Prozorov, Phys. Rev. B **79**, 134528 (2009).